GLOBAL BIOGEOCHEMICAL CYCLES, VOL. 14, NO. 3, PAGES 887-902, SEPTEMBER 2000

Radiocarbon as a diagnostic tracer in ocean and carbon cycle modeling

Thomas P. Guilderson[1]

Center for Accelerator Mass Spectrometry, Lawrence Livermore National Laboratory, Livermore, California

Kenneth Caldeira[2] and Philip B. Duffy

Climate System Modeling Group, Lawrence Livermore National Laboratory, Livermore, California

Abstract. Models which are used to study the evolution of oceanic anthropogenic CO_2 uptake in a warmer climate need to be adequately tested before their results are used to influence science and national policy, let alone predict future regional climate. In order to study circulation and the redistribution of carbon in the ocean, we have simulated the uptake and redistribution of bomb radiocarbon in a state of the art ocean general circulation model. The model does reasonably well in simulating the gross surface prebomb distribution of radiocarbon as well as some of the finer details resolved during Geochemical Ocean Section Study and World Ocean Circulation Experiment observations. In areas of downwelling the simulated surface-ocean bomb ^{14}C maxima occur too early with too much amplitude. This indicates inadequate vertical mixing and coupling between the wind driven and deeper regions of the ocean with a piling up of radiocarbon and CO_2 in the upper ocean. This inadequacy will hamper efforts to predict ocean CO_2 uptake on decadal to centennial timescales, the equivalent ventilation time of the respective water masses. These results are not specific to our model and indicate a systemic problem in many ocean models.

1. Introduction

Instrumental and climate proxy records document an increase in surface temperatures over the last ~125 years [*Houghton et al.*, 1995; *Hansen et al.*, 1996; *Mann et al.*, 1998] as well as a recent change in the frequency and intensity of El Niño-Southern Oscillation (ENSO) events [*Trenberth and Hoar*, 1996; *Rajagopalan et al.*, 1997]. A fundamental question is whether or not the observed variation in climate characteristics such as temperature or El Niño frequency is a consequence of human activities or natural variability. Understanding the (perhaps) subtle differences between natural and anthropogenic climate change relies almost exclusively on the simulation of the climate system using general circulation models (GCMs) [*Taylor and Penner*, 1994; *Santer et al.*, 1996; *Manabe and Stouffer*, 1997]. Prediction of future climate change due to increasing trace gases and, in particular, the response of the various carbon reservoirs also requires climate models [*Cao and Woodward*, 1998; *Sarmiento et al.*, 1998]. Thus climate models are important tools used to understand and predict global change.

Oceanic uptake and transport of bomb radiocarbon (as $^{14}CO_2$ created by atmospheric weapons testing) has been a useful diagnostic in ocean-only GCMs to test parameterizations of subgrid scale motions and of gas transfer between the ocean and atmosphere [e.g., *Toggweiler et al.*, 1989; 1991; *Maier-Reimer*, 1993; *Duffy et al.*, 1995; *England and Rahmstorf*, 1999]. Because of the long radioactive half-life of ^{14}C, the oceanic distribution of natural radiocarbon (^{14}C expressed as $\Delta^{14}C$ [*Stuiver and Polach*, 1977]) reflects centennial and millennial-scale circulation. Atmospheric nuclear testing in the 1950s and early 1960s resulted in an excess of ^{14}C which has augmented the natural ^{14}C gradient between surface and subsurface waters. This contrast makes the distribution of radiocarbon in the surface ocean particularly sensitive to vertical mixing. The present-day distribution of bomb radiocarbon in the ocean reflects the integration of variable circulation and air-sea exchange over the last ~40 years. We present a detailed comparison of new ocean general circulation model results with newly acquired/synthesized ^{14}C data sets. The input and ocean penetration history of bomb-radiocarbon and anthropogenic CO_2 is different, and as a consequence, bomb radiocarbon is not an exact mirror of the ocean's uptake of anthropogenic CO_2 (or heat). Thus an accepted limitation in this approach is that skill in reconstructing bomb-^{14}C in four dimensions does not necessarily imply equal skill in the prognostication of other important variables; nonetheless, poor prediction of bomb ^{14}C alert us to possible problems in predicting ocean uptake of anthropogenic CO_2.

[1] Also at Department of Earth and Planetary Sciences, Harvard University, Cambridge, Massachusetts.

[2] Also at DOE Center for Research on Ocean Carbon Sequestration, Lawrence Livermore National Laboratory, Livermore, California.

Paper number 1999GB001192.
0886-6236/00/1999GB001192$12.00

2. Model Description

Ocean model results are from the Lawrence Livermore National Laboratory's enhanced variant of the Geophysical Fluid Dynamics Laboratory Modular Ocean Model [*Pacanowski et al.*, 1991]. In the runs presented here, the model was configured with 23 layers in the vertical, 7 of which were in the upper 300 m. The model includes the equation of state as well as equations for momentum, continuity, and tracer transport. Convection is represented by an adjustment scheme which mixes vertically adjacent grid cells when the potential density of the overlying cell exceeds that of the underlying one. The model has lightly smoothed bathymetry at a resolution of 2° latitude x 4° longitude. It represents flow through all major straits except for the Strait of Gibraltar, which is accounted for with a source of salt at the appropriate depth horizon. The simulations presented here include the "Gent-McWilliams" eddy parameterization [*Gent and McWilliams*, 1990]. Coefficients of vertical diffusivity are prescribed and depend on depth. Diffusivities increase from 0.2 cm^2-sec^{-1} at the ocean surface to 1.3 cm^2-sec^{-1} at the ocean bottom. In addition to treating the physical ocean circulation, the model also calculates concentrations and fluxes of the individual carbon isotopes. The model contains a simple "Redfield" biology model [*Najjar et al.*, 1992] or more appropriately a biological chemical flux model with phosphate as the limiting nutrient. Fixation of silica by opal producers (diatoms) is allowed to outcompete calcium carbonate fixation (coccolithophorids), and as a consequence, the organic carbon to calcium carbonate rain ratio is not fixed a priori [e.g., *Maier-Reimer*, 1993]. Alkalinity is conserved and deep-sea carbonate dissolution occurs in waters that are undersaturated with respect to calcite or aragonite [*Archer*, 1991; *Maier-Reimer*, 1993]. Following the Ocean Carbon Model Intercomparison Project (OCMIP) standardization, gas exchange uses the *Wanninkhof* [1992] wind speed dependence and the solubility of *Weiss* [1974] and the model is forced with monthly climatological winds [*Hellerman and Rosenstein*, 1983]. This version of the model does not include an interactive sea-ice model. Instead, we used the climatological distribution of sea ice and sea ice inhibition of gas exchange [*Zwally et al.*, 1983]. Surface salinities and temperatures are relaxed to the observed monthly climatology [*Levitus and Boyer*, 1994] with a time constant of 60 days. The model is spun-up in an accelerated mode; it was run for 3300 surface years with an acceleration factor of 7.5 (equivalent to ~25,000 years) in the deepest model level. We used a constant zero permil atmosphere and PCO_2 of 280 μatm, to allow for deep ocean ^{14}C equilibration. This seemingly long spin-up is necessary because waters outcropping in the Southern Ocean must be returned to the deep ocean prior to complete isotopic equilibration with the atmosphere. After being spun-up, the model was then run with evolving atmospheric PCO_2 and $\Delta^{14}C$ starting in 1765 as documented by archives and observational networks [*Boden et al.*, 1993]. Similar to *Toggweiler et al.*, [1989], three zonal atmospheric bands are used for the postbomb atmospheric forcing.

Ideally, baseline $\Delta^{14}C$ values would be derived from samples prior to 1900 to avoid changes due to atmospheric weapons testing and the burning of radiocarbon-dead fossil fuel. We make a functional definition of prebomb values as those samples (water and biological archives) taken prior to 1957 and 1958 in the Northern and Southern Hemispheres, respectively. Atmospheric weapon testing had a Northern Hemisphere bias, and the mixing time between the hemispheres allows the Southern Hemisphere some small grace period, especially in the far southern latitudes where no other data currently exist. We acknowledge that Southern Hemisphere water samples may be elevated by a few per mil relative to "ideal" prebomb values.

Water samples are a discrete snapshot and may not give an accurate representation of the mean value in regions sensitive to seasonal and interannual variability. An example of this is La Jolla (LJ)-62 (0°, 130°W) taken during the El Niño of 1957 which has a value of -33‰, whereas LJ-146 taken slightly off the equator (5°N, 120°W) during the weak ENSO cold phase of 1959 has a value of -79‰ [*Bien et al.*, 1965]. In this instance, newly upwelled subsurface water has not received appreciable amounts of bomb ^{14}C even though atmospheric $\Delta^{14}C$ values have increased. Near-monthly prebomb $\Delta^{14}C$ derived from a western equatorial Pacific coral documents ~30‰ interannual extremes (1947-1957 [*Guilderson et al.*, 1998a]) and underscores the variability of prebomb $\Delta^{14}C$ in the equatorial Pacific and indeed points toward the general bias of tracer distribution snapshots from areas that are dynamic. We use as our prebomb baseline, a compilation in excess of 800 prebomb $\Delta^{14}C$ values from biological archives and early water measurements maintained at the Lawrence Livermore National Laboratory (LLNL) Center for Accelerator Mass Spectrometry (J. Southon and M. Kashgarian, manuscript in preparation, 1999). These data have been age corrected for the known age of the sample, and continuous $\Delta^{14}C$ records such as those from corals have been averaged to mean annual values. Regions that are strongly influenced by local estuarine influences (e.g., San Francisco Bay) were not included in averaging to 2°x4° bins common to the model. Measurements from within localized upwelling regions at gyre-land boundaries such as the North American coast inboard of the California Current are possibly not representative of the open gyres and may be of limited utility in a comparison with coarse resolution model results.

3. Results

3.1 General Circulation in the Model

Plate 1 depicts latitude-depth sections of simulated potential temperature and salinity, as well as meridional overturning stream function, in the Atlantic and Indo-Pacific basins. Also shown are temperatures and salinities from the

Plate 1. Zonal-average comparison of the model's simulated Atlantic and Indo-Pacific basins with *Levitus and Boyer* [1994] potential temperature (theta) and salinity and the model's meridional overturning.

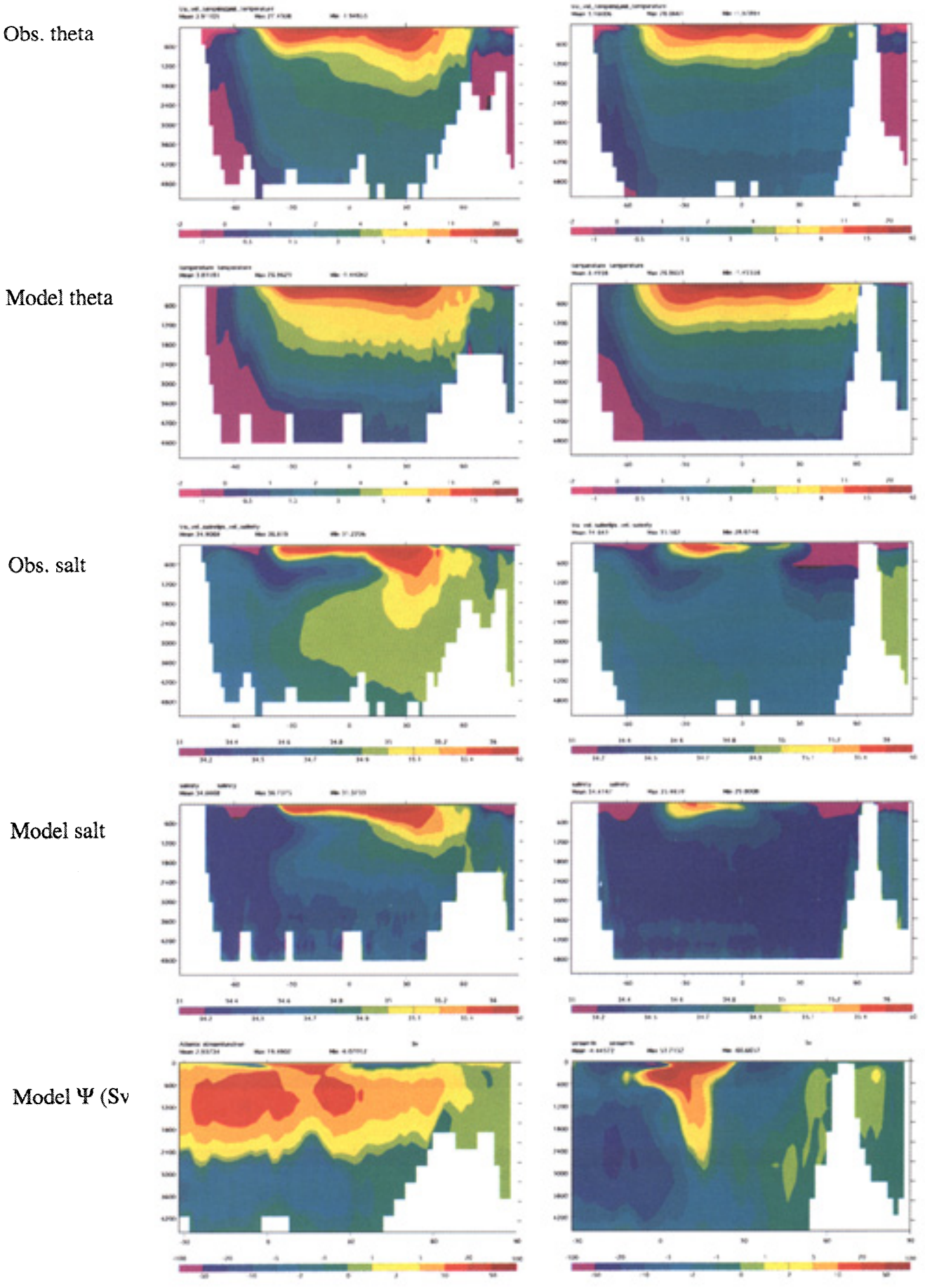
Atlantic
Indo-Pac
Obs. theta
Model theta
Obs. salt
Model salt
Model Ψ (Sv

Simulated Atlantic Ocean Section

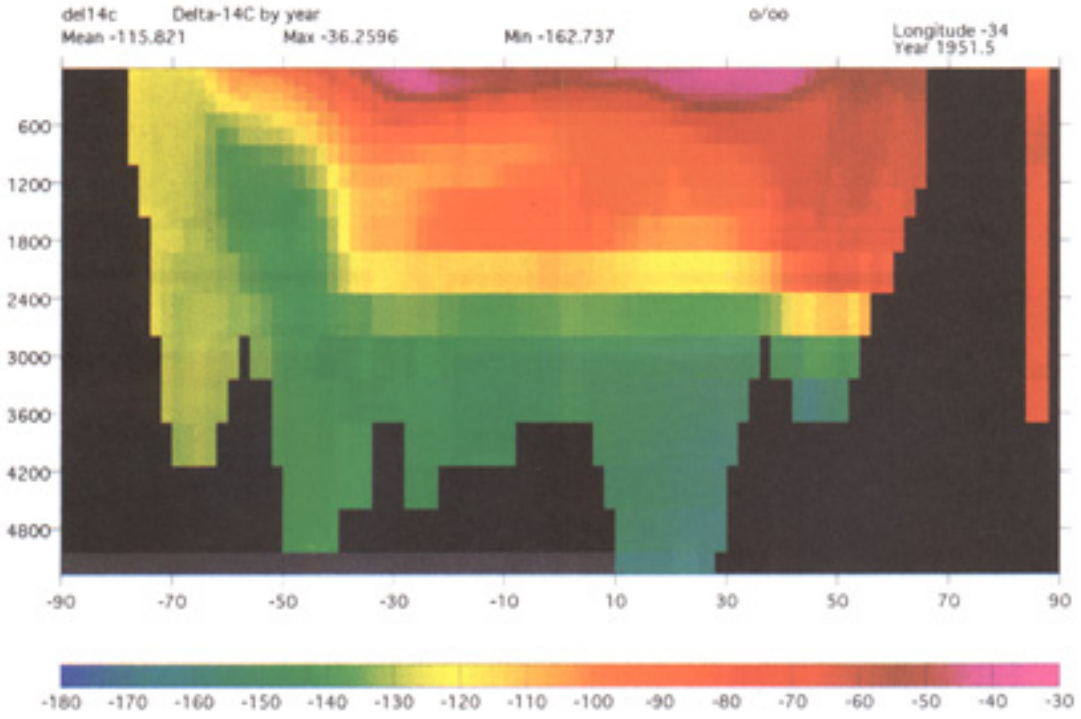

Simulated Pacific Ocean Section

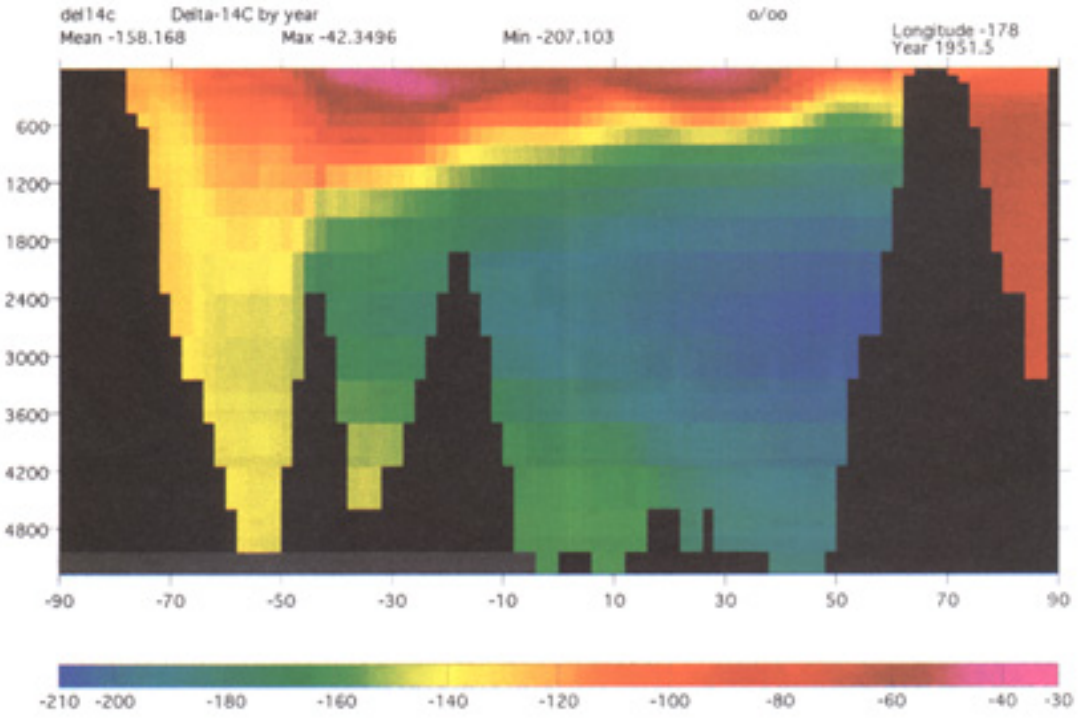

Plate 2. Simulated prebomb $\Delta^{14}C$ N-S ocean sections in the Atlantic (38°W) and along the dateline in the Pacifc.

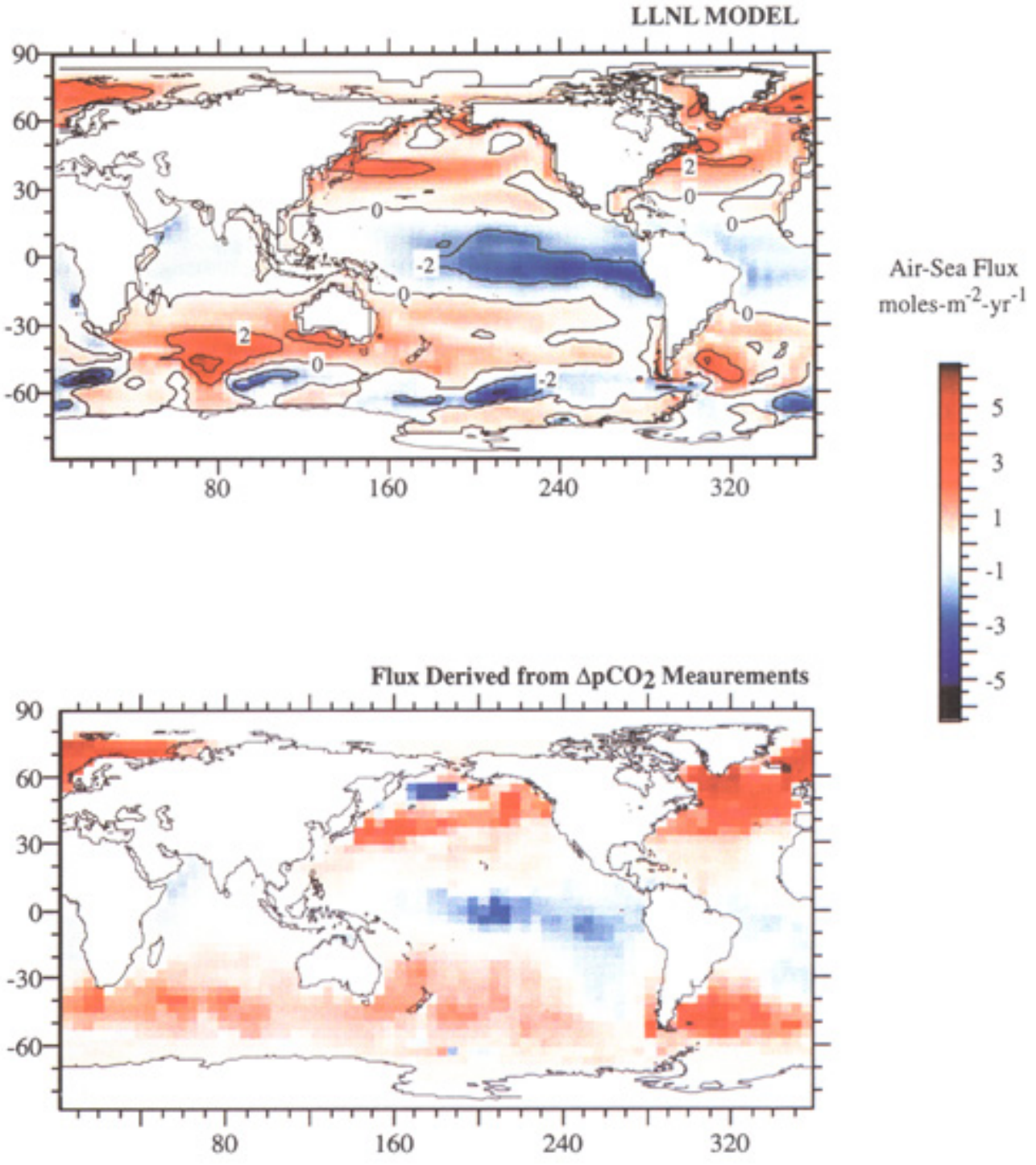

Plate 3. (a) Model annual average air-sea CO_2 flux (moles m^{-2} yr^{-1}) and (b) air-sea CO_2 flux as estimated by the ΔPCO_2 method [*Takahashi et al.*, 1997]. Although the absolute magnitude of this estimate (0.6-1.3 Gt C yr^{-1}) is low relative to the consensus value of ~2 Gt C yr^{-1}, the spatial pattern of regional sources and sinks is qualitatively accurate and agrees with model estimates.

Levitus and Boyer [1994] climatology. Perhaps the most noticeable defect in the model is the poor representation of salinity in the Southern Ocean and in the deep Atlantic and Pacific Oceans. As discussed by, for example, *Duffy and Caldeira* [1997], the overly fresh deep water results from excessive convection in the Southern Ocean. This brings deep salinities close to those in the surface Southern Ocean, which are kept fresh by the model's restoring surface boundary condition. The sections of simulated temperature show errors typical of ocean-climate models. The deep Southern Ocean and the abyssal ocean are too cold, which is another result of excessive convection under Antarctic sea ice. In both the Atlantic and Indo-Pacific basins, the thermocline is too diffuse; this is still a chronic problem in ocean-climate models despite improvements due to the use of the Gent-McWilliams eddy parameterization [*Gent and McWilliams*, 1990].

The meridional overturning stream function shows relatively weak formation of North Atlantic Deep Water (NADW), with only about 7 Sv of NADW exiting the North Atlantic Ocean. This is similar to what is obtained with similar models [e.g., *Danabasoglu and McWilliams*, 1995]. Consistent with the model's excessive Southern Ocean convection, the rate of formation of Antarctic Bottom Water (AABW) is higher (20 Sv) than the long-term estimated production of ~15 Sv [*Broecker et al.*, 1998].

Model deep water $\Delta^{14}C$ values of the various component waters are in general elevated relative to observations (Table 1) which is consistent with an over production of AABW. It has been shown to be exceedingly difficult to exactly recreate deep water $\Delta^{14}C$ in coupled models [e.g., *England and Rahmstorf*, 1999], in part owing to the inability of OGCMs to export deepwater at the correct depths (relative to observations) and difficulties in modeling subgrid scale entrainment and de-entrainment processes. A further and fundamental complication is whether or not the real-world deep ocean circulation is at steadystate [e.g., *Broecker et al.*, 1998] and if we should expect deep ocean properties which reflect centennial to millenial integrations to be accurately recreated with forcing based on recent observations [*Weaver et al.*, 1999]. Be that as it may, the model's tracer field results are exceedingly encouraging (Plate 2). Indeed, in the deep Pacific, the model recreates two distinct cores of low-^{14}C NPDW not only the previously documented core in the west [e.g., *Östlund et al.*, 1987] but also along the eastern boundary. This feature of the return circulation had gone previously unnoticed in conventional undersampled hydrographic surveys and only recently identified in the P6 (30°S) World Ocean Circulation Experiment (WOCE) radiocarbon data [*Key et al.*, 1996].

3.2 Ocean-Atmosphere CO_2 Exchange

Net oceanic uptake (in 1990) of CO_2 as represented in the model is 2±0.1 gigatons/yr (Gt C yr^{-1}). Closer examination shows significant regional sources and sinks (Plate 3a). The model has strong regional sinks in both the North Atlantic and Pacific. The tropics are a net source of CO_2 to the atmosphere, in particular the central and eastern upwelling regions of the equatorial Pacific. The model's Southern Ocean is relatively neutral, with the subtropical convergence region being a relative sink and south of the polar front zone a source. Various approaches have been used to estimate the real-world net transport flux across the air-sea boundary. The most global approach is that of the ΔPCO_2 method where the CO_2 gradient between the ocean and atmosphere is directly measured and combined with wind speed dependent gas exchange to estimate a net flux [e.g., *Tans et al.*, 1990]. The most comprehensive direct observation based estimate is that of *Takahashi et al.* [1997], who estimate a net oceanic uptake of 0.60 to 1.34 Gt C yr^{-1}. This value is substantially lower than other methods [e.g., *Quay et al.*,1992] but does not include a correction for the skin-cooling effect and riverine flux which is thought to be of the order of 1.0± 0.4 Gt C yr^{-1} (P. Quay, personal communication, 1999). The ΔPCO_2 method does have the advantage of a larger spatial coverage. Thus although quantitatively the total flux may be inaccurate, qualitatively the spatial patterns are the best available (Plate 3b). The spatial distribution of sources and sinks in the model and those determined by the ΔPCO_2 method agree quite well.

Table 1. Model Simulated Prebomb Deepwater End Member Radiocarbon Values

Water Mass	Model Value ‰	Observations ‰
L-NADW	-60	-70
CDW	-145	-165
Weddel DW	-125	-155
NPDW (47°N)	-195	-240
NPDW (38°S)	-170	-200

Observation data are derived primarily from GEOSECS as summarized by *Broecker and Peng* [1982] and rounded to the nearest 5‰.

3.3 Prebomb Surface ^{14}C

The model accurately recovers gross spatial gradients reflecting ocean dynamics (Plate 4a). Simulated and observed Southern Ocean surface $\Delta^{14}C$ values are low owing to the continuous overturning of older water which does not equilibrate with the atmosphere, in part because of seasonal sea ice coverage. The subtropics have higher $\Delta^{14}C$ in conjunction with more air-sea equilibration owing to stronger winds and the formation of mode waters. Lower $\Delta^{14}C$ values are observed in the tropics as a result of equatorial divergence and upwelling which brings low ^{14}C water to the surface. The North Atlantic drift which feeds the formation regions of North Atlantic Deep Water is adequately represented.

The model recreates to within ~10‰ the annual average prebomb surface ocean volumes in the equatorial regions and subtropics as documented by marine archives and early water measurements (Plates 4b and 4c). An exception to this is the coastal upwelling regions of eastern boundary currents (e.g., California Current) where model resolution is insufficient to accurately reproduce coastal upwelling. Model results from the Indian Ocean give the impression that the majority of upwelling occurs in the Bay of Bengal as opposed to off Arabia, but this is an artifact of advective processes. Other

areas where the model does not do as well are near Antarctica and in the subpolar North Pacific gyres.

The model's Southern Ocean $\Delta^{14}C$ values are too high by 30-40‰. This could be the result of not impeding sea ice induced air-sea $^{14}CO_2$ exchange accurately or, more likely, inaccurate overturning. As previously discussed, this version of the model has Southern Ocean convection occurring too rapidly. Model sea surface temperatures (SSTs) are too warm relative to observations which in conjunction with high $\Delta^{14}C$ indicate that there is insufficient entrainment/replacement of deeper (colder and lower $\Delta^{14}C$) water into the surface during overturning. The subpolar North Pacific is also a region of overturning and upwelling, particularly in the western North Pacific. Although deep-water values are not negative enough, the high model $\Delta^{14}C$ across the subpolar region implies unrealistic vertical mixing (too shallow and/or not enough), with the $\Delta^{14}C$ signature of newly outcropped waters advected across the remainder of the region. Galapagos $\Delta^{14}C$ is 15‰ too low and like overly cold sea surface temperatures indicates upwelling water from too deep. This is a common feature in most, if not all, coarse resolution models as well as many high-resolution models [*Mechoso et al.*, 1995; *Rodgers et al.*, 1999].

3.4. Bomb Radiocarbon

The Geochemical Ocean Sections Study (GEOSECS) provided the first quasi-global snapshot of the distribution of radiocarbon in the ocean [*Östlund and Stuiver*, 1980; *Broecker et al.*, 1985; *Östlund et al.*, 1987] in the 1970s, a feat that will not be repeated until the recently completed WOCE data become completely available. GEOSECS and WOCE radiocarbon data together with estimates of prebomb concentrations [e.g., *Broecker et al.*, 1995] provide a diagnostic of the modeled uptake and redistribution of bomb radiocarbon. Comparison of model results versus GEOSECS integrates ~20 years of circulation whereas a comparison against WOCE will integrate nearly 40 years of bomb-^{14}C uptake and redistribution. Model integrated mean bomb-^{14}C column inventories and penetration depths compare favorably with those derived from GEOSECS data [*Broecker et al.*, 1995] where observations and grid spacing overlap (compare Table 2). In the Atlantic, the 490 m mean penetration depth is biased by the model grid point equivalent to GEOSECS station 17 (75°N, 1°W) in the Norwegian Sea which in the model has convection occurring over its whole depth. Without this grid box, the mean penetration depth would be 404 m. Although the respective basin mean comparisons are encouraging, in actuality there is a distinct bias in the model simulated redistribution of bomb ^{14}C. There is over penetration in the high latitudes and not enough penetration in the temperate and subpolar regions.

Hydrographic transects made during WOCE have an increased spatial sampling density compared to comparable GEOSECS transects and affords a more direct comparison with model results along ocean sections. We compare the modeled radiocarbon distribution along 150°W in the Pacific, with that of WOCE line P16 (Plate 5) [*Key et al.*, 1996]. The model recreates the gross features and many of the details of the latitudinal-depth distribution of radiocarbon as documented by the P16 transect, although bomb radiocarbon is not penetrating deep enough in the subtropical regions, and the model's "thermocline" is too diffuse. As is often the case, the model does better in the mid latitudes and low latitudes than at the poles, failing to accurately reflect the $\Delta^{14}C$ latitudinal and vertical gradients in the subpolar regions.

Table 2. Model Simulated Mean Uptake and Redistribution of Bomb Radiocarbon at the Time of GEOSECS

	GEOSECS	Model
Atlantic		
Mean Penetration Depth, m	470	490
$\Delta\Delta^{14}C$, ‰	138	153
Column Inventory	10.05	9.44
Pacific		
Mean Penetration Depth, m	337	320
$\Delta\Delta^{14}C$, ‰	169	178
Column Inventory	8.91	8.25
Indian		
Mean Penetration Depth, m	347	336
$\Delta\Delta^{14}C$, ‰	155	148
Column Inventory	8.79	8.03

Bomb-radiocarbon penetration depth (meters), $\Delta\Delta^{14}C$ (‰), and column inventory (10^9 atoms cm^{-2}) of bomb ^{14}C as defined by *Broecker et al.* [1995]. Model averages are based on grid boxes common to the original GEOSECS stations (respective expeditions in 1972, 1973, 1974, 1977, and 1978) and are not basin-wide averages. In the model the equivalent grid box to GEOSECS station 17 (75°N, 1°W) in the Norwegian Sea has convection occuring over its whole depth (3300 m), biasing the model's mean penetration depth significantly. Without this grid box, the Atlantic basin's penenetration depth is 404 m, a more representative value for the model's Atlantic basin. Individual station/grid box comparisons can be found at the World Data Center A Boulder CO. (http://www.ngdc.noaa.gov/paleo)

3.5. Timing and Amplitude of Bomb-^{14}C Peak

The timing and amplitude of the postbomb maximum in $\Delta^{14}C$ is a diagnostic of air-sea CO_2 exchange and the mixing of bomb $^{14}CO_2$ out of the surface mixed layer and into the deeper reservoirs. A peak which occurs "early" with respect to the atmospheric forcing indicates an overly stratified upper ocean, whereas a later peak implies an advective process. With respect to amplitude, a small bomb perturbation indicates a large portion of subsurface water mixing into the surface, and a large amplitude indicates less mixing with subsurface waters. Although there may be offsets with respect to observed absolute $\Delta^{14}C$ values, matching not only the timing and amplitude of the postbomb peak but also the shape of the response function is a key test of any model trying to predict the uptake and redistribution of anthropogenic CO_2. The model predicts a postbomb as early as 1966 in the North Pacific and North Atlantic and a delayed peak (post-1995) in

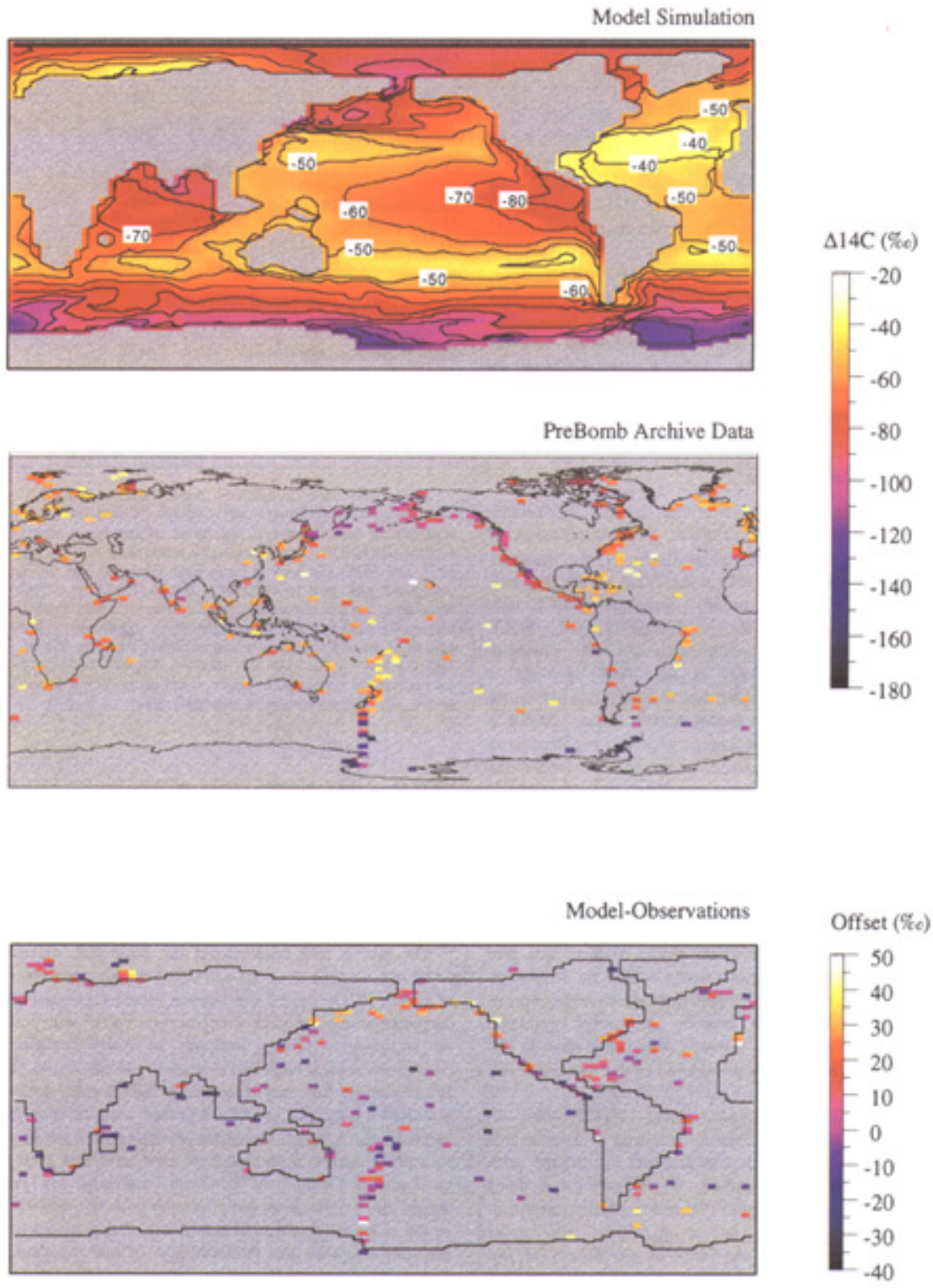
Global Pre-Bomb Δ14C Surface Ocean Synthesis
Model Simulation
-50
-40
-40
-50
-70
-80
-60
-70
-50
-50
-50
-60
PreBomb Archive Data
Δ14C (‰)
-20
-40
-60
-80
-100
-120
-140
-160
-180
Model-Observations
Offset (‰)
50
40
30
20
10
0
-10
-20
-30
-40

Table 3. Mean Annual Surface Water Prebomb to Postbomb $\Delta^{14}C$ Maxima as Recorded in Biological Archives

Location	Lat.	Lon.	Observations Year	Observations $\Delta\Delta^{14}C$ Amplitude	Ref.	OBGCM Results Year	OBGCM Results $\Delta\Delta^{14}C$ Amplitude	Observational Comments
Glover Reef, Belize	17°N	88°W	1973	209	1	1975	223	
French Frigate Shoals, Hawai'i	24°N	166°W	1971	240	2	1967	229	
Fanning Island	4°N	159°W	≥1978	171	2	1985	136	record stops in 1979
Uva Is., Gulf of Panama	8°N	82°W			2	1967	114	
Plantation Key, Florida	25°N	81°W	1975	215	3	1972	219	
North Rocks, Bermuda	32°N	65°W	1973	208	3	1972	246	
Lady Musgrage, GBR	22°S	153°E	1976	187	4	1972	181	
Heron Is, GBR	23°S	152°E	1976/80	210	4	1972	181	flat interval 1976-1980
Abrolhos Brasil	18°S	39°W	1974	193	5	1973	182	
La Paz, Sea of Cortez	24°N	110°W	1972/1989	110	6	---	---	broad flat interval 1972-1989
Urvina Bay, Galapagos	1°S	90°W	>1982	170	7	>1995	83	coral record stops in 1982
Nauru Island	1°S	166°E	1982/83	160	8	1986	143	
Guadalcanal, Solomons Is.	9°S	160°E	1975/1985	170	9	1981	150	broad flat interval 1975-1985
Rarotonga	21°S	160°W	1973	205	10	1971	210	
East Cape, New Zealand	39°S	179°E	1980	179	11	1980	183	
New South Wales, Australia	35°S	151°E	1985	151	12	1980	175	
Okinawa	26°N	127°E	1975	218	13	1972	197	
Hurghada, Egypt	27°N	34°E	1969	179	14	---	---	
Tonga	20°S	175°W	1975	>200	14	1971	202	coral record stops in 1975
Port Sudan	20°N	37°E	1976	161	14	---	---	
Viti Levu, Fiji	18°S	179°E	1974	193	14	1972	196	
Oahu, Hawai'i	21°N	158°W	1972	>220	14	1972	196	
Djibouti	12°N	43°E	1972	138	14	---	---	
Georges Bank	41°N	69°W	1974	144	15	1981	160	

Model results use the corresponding gridbox and the peak year is defined as where the first derivative of the simulated response ($\partial\Delta^{14}C/\partial T$) changes sign. Reference Key: (1) *Druffel* [1980], (2) *Druffel* [1987], (3) *Druffel* [1989], (4) *Druffel and Griffin* [1993], (5) *Druffel* [1996], (6) *Frantz et al.*, [1999], (7) *Guilderson and Schrag* [1998], (8) *Guilderson et al.* [1998a], (9) *Guilderson et al.*, [1998b], (10)*Guilderson et al.* [1999], (11) *Kalish* [1993], (12) *Kalish*, [1995], (13) *Konishi et al.* [1982], (14) *Toggweiler et al.* [1991], (15)*Weidman and Jones* [1993].

the upwelling region of the Eastern Equatorial Pacific. The amplitude of model $\Delta^{14}C$ (as $\Delta\Delta^{14}C$) ranges between 60 and 320‰ (Plate 6). A common feature in both the Atlantic and Pacific is an early simulated peak in the northern subtropic-subpolar regions with the signature advected around the respective gyre. Water samples taken in July of 1958 have a $\Delta^{14}C$ value of +25‰ at 45°N, 146°W with values decreasing toward the California coast [*Fairhall and Young*, 1985]. The high-$\Delta^{14}C$ value is a consequence of a warm, low salinity layer resulting in summer stratification (mixed layer depth 15-30 m) in the open ocean, whereas observations near the continent are much lower due to vertical mixing. Thus there is observational evidence to support a rapid increase in surface $\Delta^{14}C$ in stratified regions. However, it is unlikely that such an early peak with a widespread distribution as predicted in the model occurred in the real ocean. In the model's North Pacific, this apparent advective feature is the result of insufficient upwelling in the subpolar north Pacific and inadequate turbulent mixing at the gyre boundary. The times of the postbomb maxima are delayed and the amplitude reduced in the tropical Pacific and Atlantic and off Arabia as a consequence of the upwelling occurring in those regions. Sea-ice inhibition of gas exchange dominates the response function in the Arctic whereas in the Southern Ocean the peak is generally early.

Plate 4. (a) Model-based mean annual surface ocean prebomb (1950) values. The model was initially spun up under a 0‰ atmosphere and 280 µatmospheres PCO_2 in an accelerated mode (3300 surface years, ~25,000 deep ocean) after which atmospheric PCO_2 and radiocarbon were varied in accordance to natural archives between 1735 and 1950. (b) Surface ocean prebomb observations as compiled in the CAMS database. We make a functional definition of prebomb values as those samples (water and biological archives) taken prior to 1957 and 1958 in the Northern and Southern Hemispheres, respectively. Data are "age-corrected" for known-age of the sample and areas that have local estuarine effects (e.g., San Francisco Bay) have not been included prior to being binned to a common 2°x4° resolution for comparison with model results. (c) Difference between the model simulated prebomb surface ocean and observations. The model recreates to within ~10‰ values in the equatorial regions and subtropics but tends to be too high in the subpolar to polar regions.

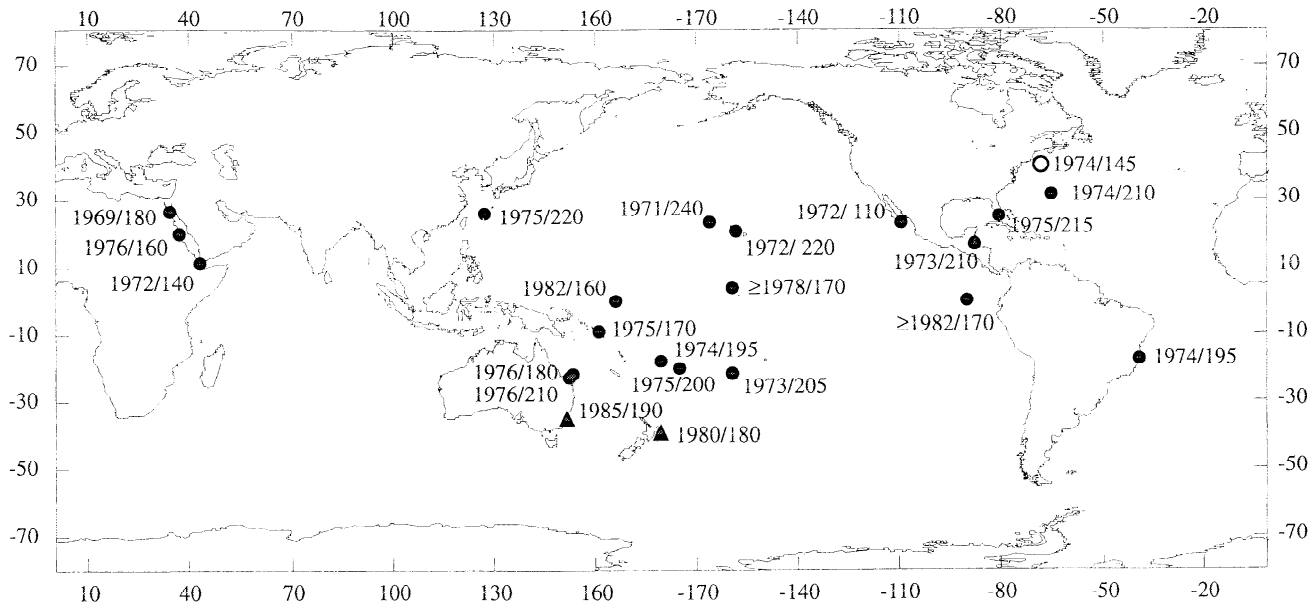

Figure 1. Observational data derived from biological archives constraining year and amplitude of the post-bomb maxima (Table 3). Data is presented as year/amplitude and rounded to the nearest 5‰. Locations where the available time series do not appear to have peaked are demarked as ≥, minimum year of post-bomb maximum and amplitude.

Observations of the postbomb maxima have better spatial coverage in the Pacific than the other major ocean basins (Table 3, Figure 1). In the Pacific the postbomb maxima occur as early as 1970 in the subpolar North Pacific to as late as 1985 on the southeast coast of Australia. Currently, available data indicate that the postbomb maxima in the eastern equatorial Pacific at Galapagos was reached after 1982, a consequence of the subsurface pathway and entrainment of significant amounts of deeper thermocline water feeding the upwelling in this region. The postbomb maxima in the western equatorial Pacific is also delayed relative to off-equatorial sites. The southernmost sites in the Southern Hemisphere show a delayed peak in response to leakage (advection) of low-^{14}C circumpolar surface water across the subtropical convergence. Pacific annual mean $\Delta\Delta^{14}C$ are between 160‰ to at least as high as 240‰. Atlantic observations document the postbomb $\Delta\Delta^{14}C$ maxima between 144 and 215‰ with timing of the peak between 1973-1975. The three sites in the Red Sea constrain the postbomb peak to 1969-1976 and amplitudes of 138-179‰.

One-dimensional modeling using a 20-box model to study ocean bomb ^{14}C exhibits consistent behavior indicating that the timing and amplitude of the surface water bomb-^{14}C maximum is insensitive to the parameterization of air-sea exchange and vertical diffusivity. Within realistic parameter space, it is impossible to significantly delay the surface postbomb maximum peak relative to the atmosphere and the canonical ~10 year isotopic equilibration time [*Broecker and Peng*, 1982]. Previous one-dimensional modeling has shown that it is difficult to reconstruct both average vertical temperature and ^{14}C profiles with realistic vertical diffusivity values [*Jain et al.*, 1996], implying that the horizontal redistribution of heat and tracer is important in the interior of the real ocean. In regions of downwelling the model's rate of $\Delta^{14}C$ increase is too fast, and the postbomb peak is early.

We compare the model's postbomb response function from three dynamically different oceanographic regimes to highlight not only inadequacies in our model but also directions for future comparisons. In the subtropics, winter radiative cooling and increased evaporation in conjunction with seasonally increasing winds result in the formation of winter "mode waters." A radiocarbon time series from the southwest subtropical Pacific [*Guilderson et al.*, 1999] reaches its postbomb maximum in 1973 with an amplitude of 205‰. Although the model's amplitude is similar (Table 3) and the postbomb peak is within a reasonable time (1971, defined by the change in slope of $\partial(\Delta^{14}C)/\partial T$), the model's response is much too fast (Figure 2a). Similar results are obtained when one compares the other available subtropical time series. The time history in the eastern equatorial Pacific (Galapagos) where the Pacific Equatorial undercurrent seasonally outcrops and where surface $\Delta^{14}C$ reflects subsurface conduits and mixing processes (Figure 2b) [*Guilderson and Schrag*, 1998]. The character of the "Galapagos" model results reflects the uptake and the dynamic redistribution of $^{14}CO_2$ of the tropical Pacific via subsurface paths, in particular the inflection points and change in the rate of increase of $\Delta^{14}C$ over time. The early rapid increase in $\Delta^{14}C$ reflects the initial air-sea exchange under rising atmospheric $\Delta^{14}C$ levels, whereas the later slower series of rises reflects the penetration of bomb ^{14}C into extratropical waters which subduct and are subsequently advected and mixed into the tropical thermocline where they then outcrop. Thus if the model were only diluting bomb ^{14}C, then only the $\Delta\Delta^{14}C$ amplitude would be dampened; to actually delay the timing of the postbomb peak requires an advective or dynamic process bringing bomb-^{14}C laden water to the surface. The western equatorial Pacific is a water mass crossroads [*Guilderson et al.*, 1998a and references therein], where higher $\Delta^{14}C$ subtropical water mixes with low-^{14}C water newly outcropped in the eastern tropical Pacific. The observed

postbomb maximum occurs in 1982/1983, delayed because of the influence of the waters advected in from the east. The model's equivalent western Pacific record (Figure 2c) records the postbomb peak in 1986 with a slightly dampened peak relative to the observated history (143 versus 160‰). Unfortunately, the correspondance in the simulated and observed profile is an artifact as the model is not recreating either the eastern equatorial Pacific nor the subtropics. Interannual variability in the tropical Pacific coral data reflects circulation changes associated with the ENSO. The model is not expected to reconstruct changes in the frequency of ENSO in part because it is forced with climatological winds and in part because the model's resolution is insufficient to adequately resolve equatorial kelvin waves, thought to be a key component of ENSO dynamics [*Zebiak and Cane*, 1987; *Graham and White*, 1988]. However, it is possible to use detailed $\Delta^{14}C$ time series from such oceanographicly dynamic regions in conjunction with higher resolution models to understand vertical and horizontal exchange processes [e.g., *Rodgers et al.*, 1999].

4. Discussion

The results presented here point to difficulties in representing dynamic processes in ocean modeling, particularly the vertical exchange between the surface and deeper waters. The distribution of $\Delta^{14}C$ (and other transient tracers) is quite sensitive to vertical exchange processes. The shape of the model's simulated surface postbomb $\Delta^{14}C$ is a fundamental diagnostic which integrates air-sea exchange and ocean dynamics. In general, the simulated surface ocean postbomb maximum occurs too early. The early postbomb peak in the subpolar and subtropical regions indicates incomplete mixing with the waters below, a fact reflected in the generally low ^{14}C-column inventories and penetration depths relative to GEOSECS. The annual mean mixed layer depth in the model is similar to that determined from oceanographic observations [*Levitus and Boyer*, 1994], and thus the early peak is likely a result of a seasonal bias in the model. The model does not have an accurate enough winter mixing to exchange ^{14}C deeper during winter overturning or storm events and in the production of "mode" waters. Not mixing deep enough has ramifications on the seasonal and spatial uptake of atmospheric PCO_2. Our model's 1990 global CO_2 uptake is 2.0 ±0.1 Gt C yr^{-1}, the "consensus" value for ocean CO_2 uptake [e.g., *Oeschger et al.*, 1975; *Broecker and Peng*, 1982, *Quay et al.*, 1992]. The spatial distribution of ocean sources and sinks (Plate 3) appears accurate with the lack of a strong southern ocean sink and the presence of a strong North Atlantic sink as documented in a variety of observational data [*Takahashi et al.*, 1995, 1997; *Sabine and Key*, 1998; *Caldeira and Duffy*, 2000]. Thus, in a global sense, the errors in the model with respect to regional CO_2 sources and sinks appear to cancel out; that is, the model returns the "consensus" value. This, however, may not be the case in attempting to predict the response of a specific region and the change in the overall net oceanic uptake in response to a warmer climate and higher atmospheric PCO_2.

Ocean model tunable parameters include vertical and horizontal eddy diffusivity. The comparison of the

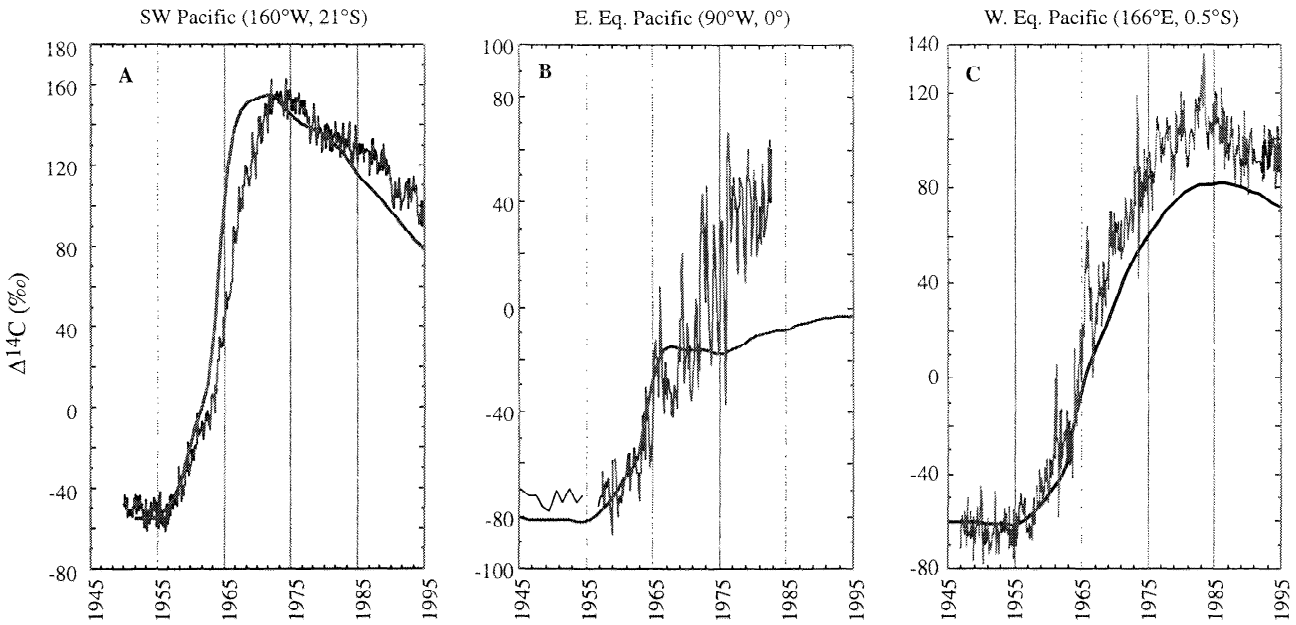

Figure 2. $\Delta^{14}C$ time evolution as measured in surface dwelling corals (thin line) in three distinct dynamic ocean regimes. (a) Rarotonga in the subtropical southwest Pacific where Ekman pumping creates downwelling (21°S, 160°W [*Guilderson et al.*, 1999]) (b) the upwelling regime of the eastern equatorial Pacific as recorded at the Galapagos (90°W, 0°; [*Guilderson and Schrag*, 1998]) and (c) the western equatorial Pacific at Nauru Island (166°E, 0.5°S; [*Guilderson et al.*, 1998]) where waters from the subtropics and the eastern tropical Pacific mix. Due to coarse resolution and climatological surface forcing, the model is not expected to recreate inter-annual variability. Model results (bold line) are from the grid box containing these locations.

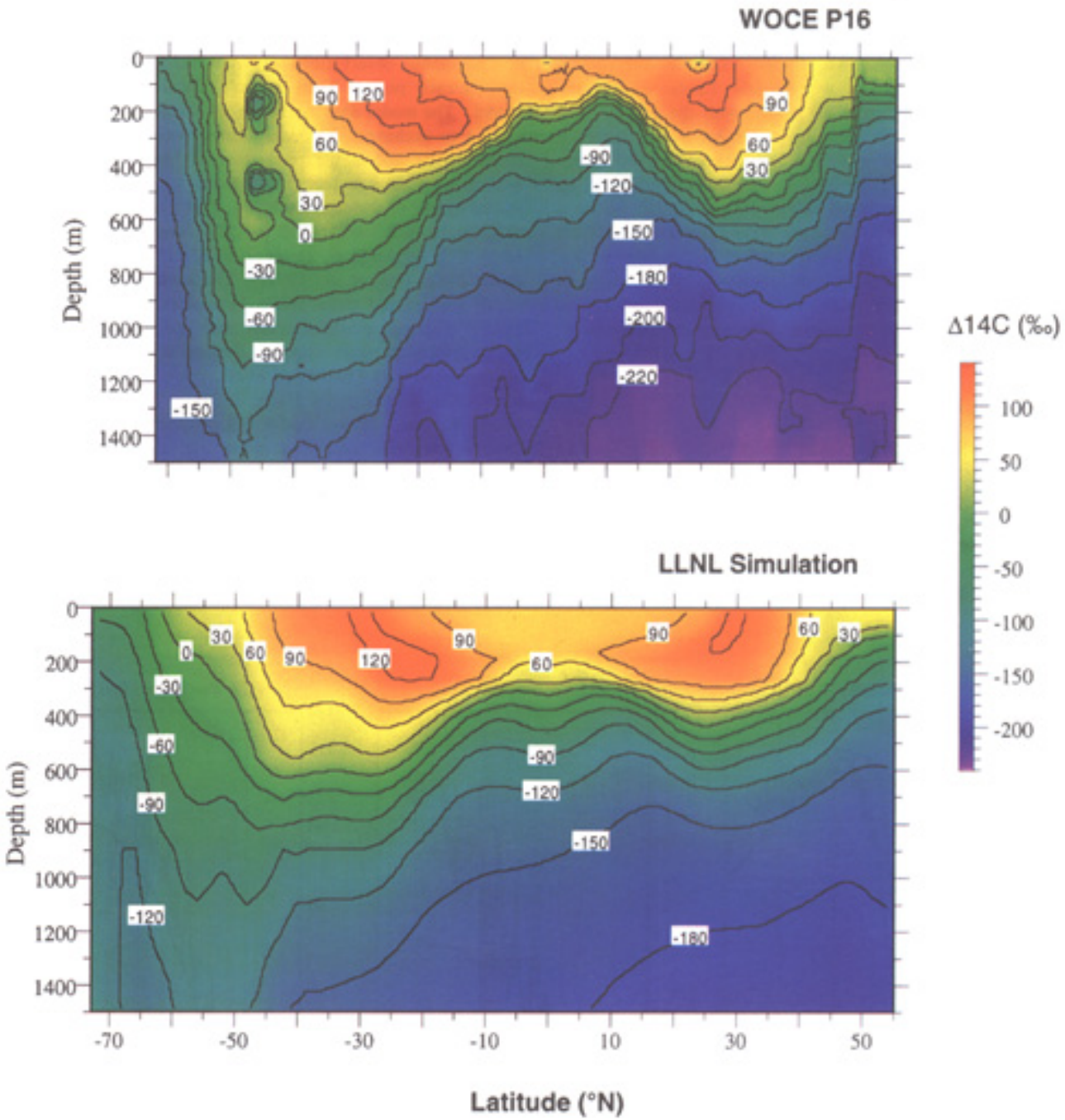

Plate 5. Simulated and observed radiocarbon profile along WOCE line P16, 150°W [*Key et al.*, 1996] in the Pacific in 1991.

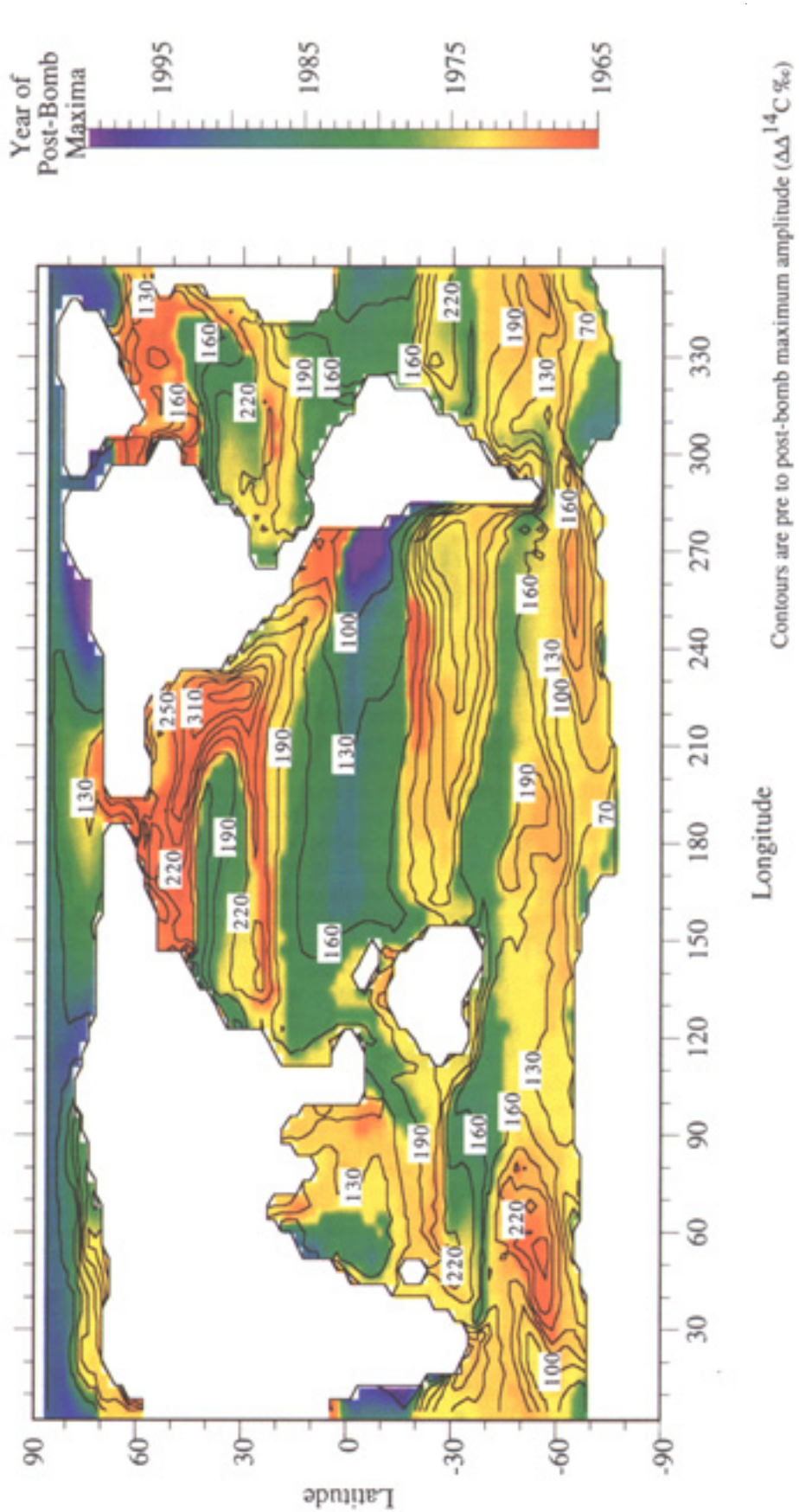

Plate 6. Year of the post-bomb maxima and amplitude ($\Delta\Delta^{14}C$) as simulated in the model. Amplitude contours are every 30‰.

distribution of temperature, salinity, and transient tracers such as $\Delta^{14}C$ can constrain chosen values to yield a more accurate representation of ocean dynamics. Since the surface forcing is different for each tracer (e.g., temperature and ^{14}C), the sensitivity of subgrid scale mixing parameterization schemes can be assessed. The currently available time-dependent radiocarbon data cannot distinguish between the Gent-McWilliams parameterization in our model versus the standard horizontal mixing [e.g., *Duffy et al.*, 1995]. In the model, there is a trade-off in the inclusion of this subgrid eddy mixing with overall vertical exchange between the surface and interior ocean. Inclusion of Gent-McWilliams relative to the standard horizontal mixing eliminates nonphysical diapycnal mixing associated with horizontal diffusion [e.g., *England and Rahmstorf*, 1999]. An associated effect is decreasing the mean penetration depth of the bomb transient and a piling up of ^{14}C (and CO_2) in surface waters. However, the interior temperatures in the model are closer to observations with Gent-McWilliams albeit a bit warmer. Compared to observations, interior temperatures between the base of the permanent thermocline and 3000 m are on average ~0.5°C too warm, and abyssal temperatures (>3500 m) are ~0.6°C too cold. The postbomb $\Delta^{14}C$ history as simulated in the model points to problems in regions which ventilate the interior of the ocean such as the subtropical regions of Ekman pumping and downwelling as well as the subtropical convergence zone of the Southern Ocean. This leads us to the fact that there is an additional fundamental bias in the model which does not accurately recover a portion of the gross interplay between the shallow wind driven and deeper buoyancy driven circulation. The regions of downwelling and interior ventilation are areas of CO_2 uptake in not only the model but the real ocean (compare Plate 3), and thus this problem will impact our ability to predict the ocean's uptake and redistribution of CO_2 on decadal to centennial timescales. This inadequacy does not appear to be specific to our model alone nor just a consequence of resolution.

5. Conclusions

The model simulated prebomb surface ocean $\Delta^{14}C$ in the temperature and tropical ocean is on average within 10‰ of observations. Regions that undergo substantial vertical exchange processes such as the Southern Ocean or the upwelling region of the eastern equatorial Pacific are not as well represented. Compared to the ~20 year integrated uptake and redistribution of bomb-^{14}C as documented by GEOSECS and *Broecker et al.*, [1995], the model's penetration depth is 3-12% too low, and integrated column inventories are also low by 5-8%. There is a systematic bias in the model's uptake of bomb ^{14}C with too much uptake at high latitudes (deep penetration depths) and not enough in temperate regions. In general, the model's postbomb maxima occurs too early. The model does well in reconstructing the depth-latitudinal $\Delta^{14}C$ of the recently completed WOCE line in the central Pacific, except for the subpolar to polar regions where the model's $\Delta^{14}C$ depth and latitudinal gradients are too small. The model also does an admirable job in reconstructing the overall depth latitudinal profiles in the respective major basins and even recovers the recently documented low-^{14}C core of NPDW along the eastern boundary [*Key et al.*, 1996], albeit absolute values tend to be 10-30‰ higher than observations. On the basis of a series of one-dimensional model experiments, the early peak in the three-dimensional ocean model does not appear to be the result of our choice of air-sea gas exchange coefficient or vertical diffusivity but rather is the result of inaccurate vertical mixing between the upper ocean and deeper reservoirs which is irrespective of the inclusion of the subgridscale eddy parameterization scheme. It is likely that part of this is the result of not propagating the effect of vertical turbulent energy fluxes resulting from intense storm activity or winter mixing. Other potentially important sub-gridscale processes which have yet to be tested are the effect of upper-ocean mesoscale eddies, modified brine rejection schemes, and spatially varying vertical diffusivities. Mesoscale eddies have the potential to move transient tracers (and nutrients) vertically in the water column along density gradients without affecting the mean density structure once the eddies themselves have passed. Improved treatment of brine can more accurately represent Southern Ocean deep water formation processes and has a significant impact on tracer distributions [*Duffy and Caldeira*, 1997; *Duffy et al.*, 1999].

The WOCE tracer results are eagerly awaited as they will represent the most systematic coverage of the ocean to date. It must be remembered that snapshots such as GEOSECS or WOCE miss the full dynamic behavior of the ocean, such that if a model "hits" GEOSECS or WOCE or returns a "consensus" ocean uptake of anthropogenic carbon it may have done so by an inaccurate pathway. The direction of coupled ocean-atmosphere modeling efforts is increasingly driven by policy with an emphasis on regional climate prediction and carbon budgets on ENSO to decadal timescales in response to rising atmospheric CO_2. As ocean model resolution increases in response to regional scale modeling and the attempt to more accurately portray the real ocean, the results will be much more sensitive to mixed layer processes and dynamics and will need to be adequately tested. Thus the need for real world data and the continued temporal evolution of tracers such as those provided by WOCE is even more important.

Acknowledgments. This manuscript benefitted from discussions with T. Brown, M. Kashgarian, K. Rodgers, C. Sabine, and J. Southon. Comments and reviews were provided by P. Quay, R. Stouffer, R. Toggweiler, and two anonymous reviewers. One-dimensional model analysis was performed by Jason Bell (UC Santa Cruz). We thank E. Druffel for recalling her early years at the La Jolla Radiocarbon Laboratory in clarifying the history of some of the water measurements performed there. The CAMS prebomb archive is maintained by J. Southon and M. Kashgarian. T. Guilderson was partially supported by grants from NSF's program in Physical Oceanography (OCE-9796253) and from Lawrence Livermore National Laboratory (98-ERI-002). This work was performed under the auspices of the U.S. Department of Energy by Lawrence Livermore National Laboratory (contract W-7405-Eng-48). Supplementary information will be archived at WDC-A, Boulder CO (http://www.ngdc.noaa.gov/paleo/).

References

Archer, D., Modeling the calcite lysocline, *J. Geophys. Res.*, *96*, 17,037-17,050, 1991.

Bien, G. S., N. W., Rakestraw, and H. E. Suess, Radiocarbon in the Pacific and Indian Oceans and its relation to deep water movements, *Limnol., Oceanogr.*, *10*, R25-R37, 1965.

Boden, T.A., D.P. Kaiser, R.J. Sepanski, and F.W. Stoss, (Ed.). Trends

'93: A Compendium of Data on Global Change, *Publ. ORNL/CDIAC-65*, Carbon Dioxide Inf. Anal. Cent., Oak Ridge Nat. Lab. Oak Ridge, Tenn., 1994.

Broecker, W. S., and T-H. Peng, *Tracers in the Sea.*, 690 pp., Lamont-Doherty Geological Observatory Press, Palisades, N.Y., 1982.

Broecker, W. S., T-H. Peng, G. Östlund, and M. Stuiver, The distribution of bomb radiocarbon in the ocean, *J. Geophys. Res., 90*, 6953-6970, 1985.

Broecker, W.S., et al., Oceanic radiocarbon: Separation of the natural and bomb components, *Global Biogeochem. Cycles, 9*, 263-288, 1995.

Broecker, W.S., et al., How much deep water is formed in the Southern Ocean?, *J. Geophys. Res., 103*, 15,833-15,843, 1998.

Caldeira, K., and P.B. Duffy, The role of the Southern Ocean in uptake and storage of anthropogenic carbon dioxide, *Science, 287*, 620-622, 2000.

Cao, M., and F. I. Woodward, Dynamic responses of terrestrial ecosystem carbon cycling to global climate change, *Nature, 393*, 249-252, 1998.

Danabasoglu, G., and J.C. McWilliams, Sensitivity of the global ocean circulation to parameterizations of mesoscale tracer transports, *J. Clim. 8*, 2967-2987, 1995.

Druffel, E.R.M., Radiocarbon in annual coral rings of the Pacific and Atlantic oceans, Ph.D. thesis, 213 pp., Univ. of Calif., San Diego, 1980.

Druffel, E.R.M., Bomb radiocarbon in the Pacific: Annual and seasonal timescale variations, *J. Mar. Res., 45*, 667-698, 1987.

Druffel, E.R.M., Variability of ventilation in the North Atlantic determined from high precision measurements of bomb radiocarbon in banded corals, *J. Geophys. Res., 94*, 3271-3285, 1989.

Druffel, E. R. M., Post-bomb radiocarbon records of surface corals from the tropical Atlantic Ocean *Radiocarbon, 38*, 563-572, 1996.

Druffel, E. R. M., and S. Griffin, Large variations of surface ocean radiocarbon: Evidence of circulation changes in the southwestern Pacific, *J. Geophys. Res., 98*, 20,249-20,260, 1993.

Duffy, P.B., and K. Caldeira, Three-dimensional model calculation of ocean uptake of bomb ^{14}C and implications for the global budget of bomb ^{14}C, *Global Biogeochem. Cycles, 9*, 373-375, 1995.

Duffy, P.B., and K. Caldeira, Sensitivity of simulated salinity in a three-dimensional ocean model to upper-ocean transport of salt from sea-ice formation, *Geophys. Res. Lett., 24*, 1323-1326, 1997.

Duffy, P. B., D. E. Eliason, A. J. Bourgois, and C. C. Covey, Simulation of bomb radiocarbon in two global general circulation models, *J. Geophys. Res., 100*, 22,545-22,564, 1995.

Duffy, P.B., M. Eby, and A.J. Weaver, Effects of sinking of salt rejected during formation of sea ice on results of an ocean-atmosphere-sea ice climate model, *Geophys. Res., Lett., 26*, 1739-1742, 1999.

England, M.H., and S. Rahmstorf, Sensitivity of ventilations rates and radiocarbon uptake to subgrid-scale mixing in ocean models, *J. Phys. Oceanog.*, in press, 1999.

Fairhall, A. W., and A. W. Young, Historical ^{14}C mesurements from the Atlantic, Pacific and Indian Oceans, *Radiocarbon, 27*, 473-507, 1985.

Frantz, B., M. Kashgarian, M.S. Foster, and K. Coales, Growth rate and potential climate record from a rhodolith using ^{14}C AMS, *EOS Trans. AGU., 80*, Spring Meet. Suppl. S176, 1999.

Gent, P. R., and J. C. McWilliams, Isopycnal mixing in aocean general circulation models, *J. Phys. Oceanogr., 20*, 150-155, 1990.

Graham, N.E., and W.B., White, The El Niño Cycle: A natural oscillator of the Pacific ocean-atmosphere system, *Science, 240*, 1293-1301, 1988.

Guilderson, T.P., and D.P. Schrag, Abrupt shift in subsurface temperatures in the Eastern Tropical Pacific associated with recent changes in El Niño, *Science, 281*, 240-243, 1998.

Guilderson, T.P., D.P. Schrag, M. Kashgarian, and J. Southon, Radiocarbon variability in the western equatorial Pacific inferred from a high-resolution coral record from Nauru Island, *J. Geophys. Res., 103*, 24,641-24,650, 1998a.

Guilderson, T.P., D.P. Schrag, J. Southon, and M. Kashgarian, Identifying shallow circulation pathways in the tropical Pacific using radiocarbon in corals, *EOS Trans. AGU, 79*, Fall Meet. Suppl. F483, 1998b.

Guilderson T.P., et al., Southwest subtropical Pacific surface water radiocarbon in a high-resolution coral record, *Radiocarbon*, in press, 1999.

Hansen, J., R. Reudy, M. Sato, and R. Reynolds, Global surface air temperature in 1995: Return to pre-Pinatubo level, *Geophys. Res. Lett., 23*, 1665-1668, 1996.

Hellerman, S., and M. Rosenstein, Normal monthly wind stress over the world ocean with error estimates, *J. Phys. Oceanogr., 13*, 1093-1104, 1983.

Houghton, J. T., G. J. Jenkins, and J. J. Ephraums, *Climate Change, The IPCC Scientific Assessment*, Cambridge Univ. Press, 364 pp., New York, 1995

Jain, A. K., H. S. Kheshgi, M. I. Hoffert, and D. J. Wuebbles, Distribution of radiocarbon as a test of global carbon cycle models, *Global Biogeochem. Cycles, 9*, 153-166, 1995.

Joussaume, S. and K.E. Taylor, Status of the Paleoclimate Modeling Intercomparison Project (PMIP), in *Proceedings of the First International AMIP Scientific Conference* (edited by W. L. Gates), pp. 425-430, World Climate Research Program, Geneva Switzerland, 1995.

Kalish, J. M., Pre-and post-bomb radiocarbon in fish otoliths, *Earth Planetary Sci. Lett., 114*, 549-554, 1993.

Kalish, J. M., Application of the bomb radiocarbon chronometer to the validation of redfish Centroberyx affinis age, *Can. J. Aquat. Sci., 52*, 1399-1405, 1995.

Key, R. M., et al., WOCE AMS radiocarbon I: Pacific Ocean results (P6, P16, and P17), *Radiocarbon, 38*, 425-518, 1996.

Konishi, K. J., T. Tanaka, and M. Sakanoue, Secular variation of radiocarbon concentration in seawater: A sclerochronological approach, in *Proc. Fourth Intl. Coral Reef Symp.*, vol. 1, edited by E. D. Gomez, pp. 181-185, Mar. Sci. Cent., Univ. of the Philippines, Manila, 1982.

Levitus, S., and T. Boyer, *World Ocean Atlas 1994*, vol. 4, 117 pp., Natl. Oceanic and Atmos. Admin., U.S. Dep. of Commer., Washington, D.C., 1994.

Maier-Reimer, E., Geochemical cycles in an ocean circulation model: Preindustrial tracer distributions, *Global Biogeochem. Cycles, 7*, 645-678, 1993.

Manabe, S., and R. J. Stouffer, Climate variability of a coupled ocean-atmosphere-land surface model: Implication for the detection of global warming - The Walter Orr Roberts lecture, *Bull. Am. Meteorol. Soc., 78*, 1177-1185, 1997.

Mann, M. E., R. S. Bradley, and M. K. Hughes, Global-scale temperature patterns and climate forcing over the past six centuries, *Nature, 392*, 779-787, 1998.

Mechoso, C.R., et al., The seasonal cycle over the tropical Pacific in coupled ocean-atmosphere general circulation models, *Mon. Weather Rev., 123*, 2825-2838, 1995.

Najjar, R. G., J. L., Sarmiento, and J. R. Toggweiler, Downward transport and fate of organic matter in the ocean: Simulations with a general circulation model, *Global Biogeochem. Cycles, 6*, 45-76, 1992.

Oeschger, H., U. Siegenthaler, and A. Gugelmann, Box diffusion model to study carbon dioxide exchange in nature, *Tellus, 27*, 168-192, 1975.

Östlund, G., and M., Stuiver, GEOSECS Pacific radiocarbon, *Radiocarbon, 22*, 25-53, 1980.

Östlund, H. G., H. Craig, W. S. Broecker, and D. Spencer, *GEOSECS Atlantic, Pacific, and Indian Ocean Expeditions*, vol. 7, 200 pp., Natl. Sci. Found., Washington, D.C., 1987.

Pacanowski, R. K., K. Dixon, and A. Rosati, The GFDL Modular Ocean Model Users Guide, v 1.0, *GFDL Ocean Group Tech. Rep. 2*, Geophys. Fluid Dyn. Lab., Princeton, N.J., 1991.

Quay, P., B. Tilbrook, and C.S. Wong, Oceanic uptake of fossil fuel CO_2: Carbon-13 evidence, *Science, 256*, 74-79, 1992.

Rajagopalan, B., U. Lall, and M.A. Cane, Anomalous ENSO occurrences: An alternate view, *J. Clim. 10*, 2351-2357, 1997.

Rodgers, K.B., D.P. Schrag, M.A. Cane, and N.H. Naik, The bomb-14C transient in the Pacific ocean, *J. Geophys. Res.*, 105, 489-512, 2000.

Sabine. C. L., and R. M. Key, Looking for fossil fuel in the oceans, 1998 U. S. WOCE Report, *U. S. WOCE Implementation Rep. 10*, pp. 26-29,College Station TX, 1998.

Santer, B., et al., A search for human influences on the thermal structure of the atmosphere, *Nature , 382*, 39-46, 1996.

Sarmiento, J. L., T. M. C. Hughes, R. J. Stouffer, and S. Manabe, Simulated response of the ocean carbon cycle to anthropogenic climate warming, *Nature*, *393*, 245, 1998.

Stuiver, M., and H. A. Polach, Discussion and reporting of ^{14}C data, *Radiocarbon*, *19*, 355-363, 1977.

Takahashi, T., et al., Global air-sea flux of CO2: An estimate based on measurements of sea-air pCO_2 difference, *Proc. Natl. Acad. Sci.*, *94*, 8292-8299, 1997.

Tans, P.P., I.Y. Fung, and T. Takahashi, Observational constraints on the global atmospheric CO_2 budget, *Science*, *247*, 1431-1438, 1990.

Taylor, K.E., and J.E. Penner, Response of the climate system to atmospheric aerosols and greenhouse gases, *Nature*, *369*, 734-737, 1994.

Toggweiler, J.R., K. Dixon, and K. Bryan, Simulations of Radiocarbon in a Coarse-Resolution World Ocean Model, 2, Distributions of bomb-produced 14C, *J. Geophys. Res.*, *94*, 8243-8264, 1989.

Toggweiler, J. R., K. Dixon, and W. S. Broecker, The Peru upwelling and the ventilation of the South Pacific thermocline, *J. Geophys. Res.*, *96*, 20467-20497, 1991.

Trenberth, K.E., and T.J. Hoar, The 1990-1995 El Niño- Southern Oscillation event: Longest on record. *Geophys. Res. Lett.*, *23*, 57-60, 1996.

Wanninkhof, R., Relationship between wind speeds and gas exchange over the ocean, *J. Geophys. Res.*, *97*, 7373-7382, 1992.

Weaver, A.J., et al., On the evaluation of ocean and climate models using present-day forcing, *Atmos. Ocean*, in press, 1999.

Weidman, C., and G. Jones, A shell-derived time history of bomb ^{14}C on Georges Bank and its Labrador Sea implications, *J. Geophys. Res.*, *98*, 14577-14588, 1993.

Weiss, R. F., Carbon dioxide in water and seawater: the solubility of a non-ideal gas, *Mar. Chem.*, *2*, 203-215, 1974.

Zebiak, S. E., and M.A. Cane, A Model El Niño-Southern Oscillation. *Mon. Weather Rev.*, *115*, 2262-2278, 1987.

Zwally, H. J. et al., Antarctic Sea Ice, 1973-1976: Satellite Passive Microwave Observations, 206 pp., NASA, Washington D.C., 1983.

K. Caldeira and P.B. Duffy, Climate System Modeling Group, Lawrence Livermore National Laboratory, L-103, 7000 East Avenue, Livermore, CA 94551.

T.P. Guilderson, Center of Accelerator Mass Spectrometry, Lawrence Livermore National Laboratory, L-397, 7000 East Avenue, Livermore, CA 94551. (guilderson1@popeye.llnl.gov)

(Received June 22, 1999; revised October 19, 1999; accepted November 3, 1999).